A Multiphysics Computational Technique for THz-Frequency Characterization of Semiconductors and Metals

Keely Willis, *Irena Knezevic*, and *Susan C. Hagness*
University of Wisconsin-Madison, 1415 Engineering Drive, Madison, WI 53706, USA.
keelywillis@gmail.com, knezevic@engr.wisc.edu, and hagness@engr.wisc.edu

Abstract

We present a multiphysics computational technique for calculating the THz-frequency conductivity in semiconductors and metals. This novel technique combines the ensemble Monte Carlo (EMC) simulation of carrier transport with the finite-difference time-domain (FDTD) solver of Maxwell's curl equations and the molecular dynamics (MD) technique for describing short-range Coulomb interactions between particles with finite radii and the exchange interaction between indistinguishable electrons. The calculated complex conductivity of doped bulk silicon shows excellent agreement with experimental data. This work represents the first comprehensive computational technique for THz-regime characterization of materials with relatively high carrier densities.

1 Introduction

Doped semiconductors and metals typically have both plasma frequency, $\omega_{\rm p}$, and characteristic carrier scattering rate, τ^{-1}, in the terahertz (THz) frequency regime [1]. In this regime, the stimulating frequency ω approaches τ^{-1}, and conductivity becomes strongly frequency-dependent [1]. Under these circumstances, the Drude model, which relates the frequency-dependent conductivity, $\sigma(\omega) = \sigma_0/(1 - i\omega\tau)$, to the dc conductivity σ_0, loses validity. Materials that are well-described by the Drude model in the neighboring optical and microwave frequency regimes must be independently characterized for THz frequencies. The lack of inexpensive, convenient sources for THz radiation has left this frequency range relatively under-explored [2]. Even a technologically important material like silicon is not well characterized in this regime [1, 3]. This gap in our understanding of THz-frequency materials properties is the driving force behind the development of a comprehensive simulation technique for carrier dynamics under THz-frequency stimulation in conducting materials.

The ensemble Monte Carlo (EMC) technique accurately describes carrier dynamics in the diffusive regime through a stochastic solution of the Boltzmann transport equation [4]. State-of-the-art EMC implementations typically incorporate electric field effects with simple quasielectrostatic solvers. At THz frequencies, where the dynamic interaction of carriers and fields depends strongly on radiation frequency, quasielectrostatic analyses lose accuracy [3]. The finite-difference time-domain (FDTD) technique is a fully electrodynamic computational technique that calculates electric and magnetic fields according to grid-based solutions of the time-dependent Maxwell's curl equations [5]. Although FDTD implementations usually describe electromagnetic systems that are uniformly charge-neutral, FDTD analysis with nonuniform charge density has been employed within the particle-in-cell (PIC) technique for computational plasma physics. The typical PIC implementation describes systems with carrier densities, n_0, below 10^{15} cm^{-3}, in which the average spacing between charged particles is large and short-range interactions have little effect on particle dynamics [6].

In metals and semiconductors with $n_0 > 10^{16}$ cm^{-3}, the short-range Coulomb force between charged particles significantly effects materials properties [7]. At carrier densities above 10^{19} cm^{-3}, the exchange interaction between indistinguishable electrons can significantly effect bulk materials properties as well [8]. FDTD accurately describes the long-range Coulomb force, and suppresses the short-range Coulomb force between particles closer than the FDTD grid cell [9]. The molecular dynamics (MD) technique describes the Coulomb interaction among charged particles according to an analytical description of the force between each pair of particles. MD has been extended to describe the exchange interaction between indistinguishable electrons [8].

In this paper, we present the EMC/FDTD/MD method for THz-frequency characterization of semiconductors and metals. This comprehensive computational technique provides a fully electrodynamic description of particle dynamics with full Coulomb interaction. We use MD to describe the strong forces between charges separated by distances smaller than the computational grid cell, via a modified form of the corrected-Coulomb scheme [7]. With the addition of MD, the solver is extended to high-conductivity semiconductors and metals. The combined solver is described in Sec. 2, with details on the MD-implementation of the exchange interaction and the finite dopant-ion radius [8, 10]. Section 3 demonstrates the use of the solver to calculate the complex conductivity of doped silicon

978-1-4244-6051-9/11/$26.00

at two doping densities. The complex conductivity calculated by EMC/FDTD/MD shows excellent agreement with published experimental data.

2 Combined EMC/FDTD/MD solver

In this technique, the three constituent solvers interact at every time step to describe carrier dynamics under applied electromagnetic stimulation. Electromagnetic fields from FDTD and MD accelerate EMC carriers according to the Lorentz force. Microscopic currents from EMC carrier motion influence FDTD fields, and instantaneous carrier positions define the direct Coulomb force and the exchange interaction in MD.

We define a 3D FDTD computational domain with the dielectric constant of the material of interest, ϵ_{r}, specified throughout (Fig. 1). The multiphysics EMC/FDTD/MD region, enclosed by the white rectangle in Fig. 1, is embedded within the larger FDTD domain. This coupled region extends over the full height of the FDTD domain. Domain boundaries normal to z are treated with periodic boundary conditions in all three solvers, permitting unrestricted carrier motion and continuous Coulomb interaction in z. The FDTD domain boundaries normal to x and y are treated with convolutional perfectly-matched layer (CPML) absorbing boundary conditions [5], allowing finite-grid representation of an infinite space. EMC enforces specular reflection of carriers from the $x-$ and $y-$normal boundaries of the multiphysics region. THz-frequency electromagnetic plane waves are introduced via the total-field scattered-field (TFSF) formulation with wavevector in x and polarization in z.

FDTD fields satisfy Gauss's law if the initial field distribution satisfies Gauss's law, and if the continuity equation is enforced [11]. We initialize the electric fields to satisfy Gauss's law according to a numerical solution to Poisson's equation for the initial charge distribution. The current density is calculated to enforce current continuity according to the Villasenor-Buneman scheme [3]. An important advantage of the explicit enforcement of the continuity equation, and thereby the implicit satisfaction of Gauss's law, is that the long-range Coulomb interaction among carriers is automatically accounted for during the simulation.

The classical MD implementation, which treats electrons and ions as δ-functions of charge [7], accurately describes the Coulomb interaction in bulk materials with $n_0 < 10^{16}$ cm^{-3}. At these low carrier densities, charged particle interactions are well-represented by a fully classical description. At high carrier densities, dopant ions are more accurately represented with a finite radius [10]. Above $n_0 = 10^{18}$ cm^{-3}, the exchange interaction between

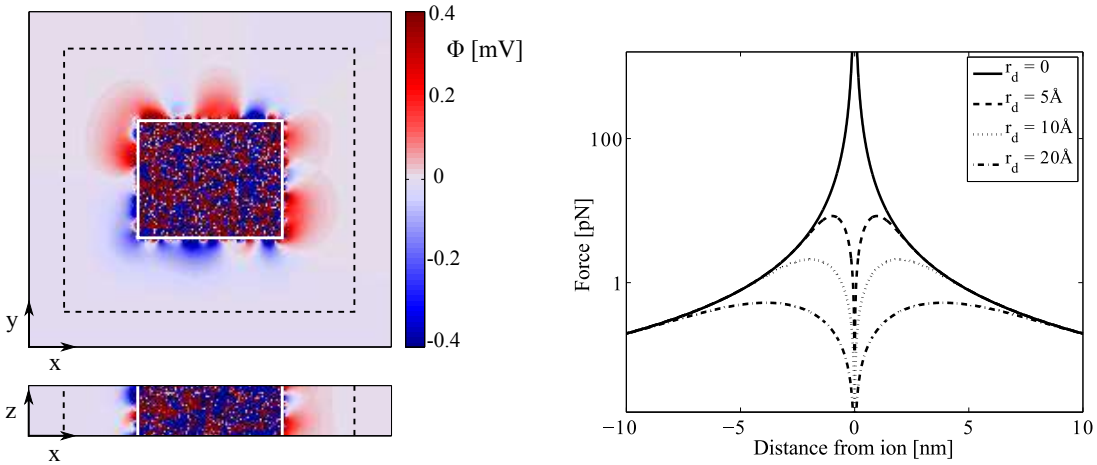

Figure 1: (a) Cross-sectional slices of the initial electrostatic potential Φ throughout the computational domain in the absence of external excitation. The white box encloses the region in which the EMC, FDTD and MD simulations are combined. Φ varies rapidly within the coupled region due to random placement of electrons and ions. The black dashed lines indicate the location of the TFSF boundary. (b) Electrostatic force acting on an electron as a function of distance from an ion of finite radius r_{d}.

indistinguishable particles increasingly impacts materials properties [8]. We describe the exchange interaction with MD according to the formulation of Ref. [8]. Carriers are defined as Gaussian wave packets with a finite radius r_{c}; the wavefunction of the i^{th} electron is as follows:

$$\phi_{\vec{p}_i}(\vec{r}_i) = (2\pi r_c^2)^{-3/4} \exp\left(-\frac{\vec{r}_i^2}{4r_c^2} + i\vec{k}_i \cdot \vec{r}_i\right). \quad (1)$$

The wave packet probability density is significant only within a few r_{c} of the electron's assumed position $\vec{r}_{\mathrm{i}}$ and a few $\hbar/2r_{\mathrm{c}}$ of the assumed momentum $\vec{p}_{\mathrm{i}} = \hbar\vec{k}_{\mathrm{i}}$. The resulting force on an electron is precalculated according to the method described in Ref. [8], and stored in look-up tables. The dopant-ion charge is analogously described with a Gaussian profile of characteristic half-width r_{d}. Figure 1(b) shows the magnitude of the force acting on an electron as the electron is swept past an ion with radius r_{d}, for several values of r_{d}. As r_{d} increases, the total force on the electron decreases.

The effective linear-regime complex conductivity $\hat{\sigma}$ is computed from the FDTD electric fields and the EMC current densities as described in Ref. [11]. To determine the dc conductivity, we specify TFSF currents that ramp up smoothly from zero to the desired constant level to source a dc electric field in the main grid. We calculate the dc conductivity $\hat{\sigma}(0)$ as a function of r_{c} and r_{d}. In order to determine the optimal values of r_{c} and r_{d}, r_{c} was varied between the classical approximation of 0 Å and the exchange-hole radius given by the Hartree-Fock theory [12]. Similarly, r_{d} was varied between the classical approximation of 0 Å and the effective Bohr radius for the dopant of interest (for example, the effective Bohr radius of a phosphorous ion in silicon is 13.8 Å) [13]. By comparing $\hat{\sigma}(0)$ with the known dc conductivity σ_0, we determine appropriate values for r_{c} and r_{d}. Once these radii are known, we may use EMC/FDTD/MD to predict the THz conductivity of the material of interest.

3 Example: THz-conductivity of doped silicon

In this section we demonstrate the accuracy of EMC/FDTD/MD by comparing the calculated $\hat{\sigma}$ with published experimental data for doped silicon at THz frequencies [1]. The dielectric constant is $\epsilon_r = 11.7$ throughout the FDTD computational domain and in MD calculations. EMC scattering rates are calculated for room-temperature doped silicon [4]. Figure 2 shows the comparison of experimental and numerical data for two samples of $n-$type silicon. The material in Fig. 2(a) has a dc resistivity of 8.15 Ω cm, corresponding to $n_0 = 5.47 \times 10^{14}$ cm^{-3}. Physical considerations and dc conductivity calculations give $r_c = 426$ Å and $r_d = 1$ Å. The numerical prediction for conductivity shows excellent agreement with experiment. The Drude-model conductivity, calculated with the stated doping density and corresponding low-field mobility, differs significantly from both numerical and experimental data.

Figure 2(b) shows silicon with a dc resistivity of 0.21 Ω cm, corresponding to $n_0 = 3.15 \times 10^{16}$ cm^{-3}. Physical considerations and dc conductivity calculations give $r_c = 110$ Å and $r_d = 2.5$ Å. EMC/FDTD/MD results for the real part of $\hat{\sigma}$ show excellent agreement with experiment. The numerical values for the imaginary part of $\hat{\sigma}$ do not agree quite as well with experiment, though the trend of calculated $\hat{\sigma}$ is the same as that of the experimental results. The imaginary part of the conductivity describes the phase shift between $\vec{E}$ and $\vec{J}$, and as a result Im($\hat{\sigma}$) is highly susceptible to small errors in both the computational and experimental systems. FDTD numerical dispersion could contribute to this error. In the experimental characterization, small inaccuracies in the measured thickness of the sample would also manifest as error in Im($\hat{\sigma}$) [1].

4 Conclusion

We have presented the EMC/FDTD/MD method for THz-frequency characterization of materials with a broad range of carrier densities. The technique provides a fully electrodynamic description of carrier dynamics with full Coulomb interactions. Electrons and ions are treated with finite radii, and a method to determine these radii has been presented. The comparison with experimental data demonstrates the accuracy of EMC/FDTD/MD as a predictive tool for THz-frequency conductivity of materials.

5 Acknowledgments

This work was supported by the Air Force Office of Scientific Research, award number FA9550-08-1-0052.

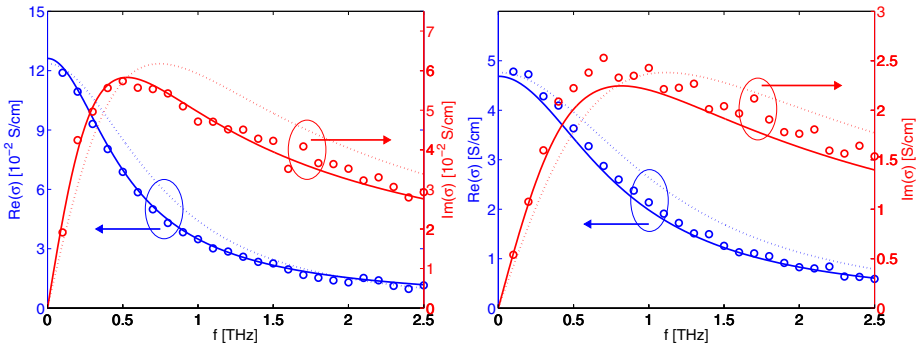

(a) (b)

Figure 2: THz conductivity of n-type silicon, comparison of experimental data with 3D EMC/FDTD/MD results. (a) $n_0 = 5.47 \times 10^{14}$ cm^{-3}, $r_c = 426$ Å and $r_d = 1$ Å. (b) $n_0 = 3.15 \times 10^{16}$ cm^{-3}, $r_c = 110$ Å and $r_d = 2.5$ Å. The dotted line shows the Drude model prediction for the conductivity, based on the known doping density and mobility of the material. The solid line indicates the analytical fit to the experimental data. $\hat{\sigma}$ calculated by EMC/FDTD/MD is shown with open circles. The numerical data demonstrates excellent agreement with the experimental conductivity. The Drude model prediction differs significantly from both.

References

[1] T. I. Jeon and D. Grischkowsky. Nature of conduction in doped silicon. *Phys. Rev. Lett.*, 78(6):1106–1109, 1997.

[2] J. H. Booske. Plasma physics and related challenges of millimeter-wave-to-terahertz and high power microwave generation. *Phys. Plasmas*, 15, 2008.

[3] K. J. Willis, J. Ayubi-Moak, S. C. Hagness, and I. Knezevic. Global modeling of carrier-field dynamics in semiconductors using EMC-FDTD. *J. Comput. Electron.*, 8:153–171, 2009.

[4] C. Jacoboni and P. Lugli. *The Monte Carlo Method for Semiconductor Device Simulation*. Springer-Verlag, New York, 1989.

[5] A. Taflove and S. C. Hagness. *Computational Electrodynamics: The Finite-Difference Time-Domain Method*. Artech House, 3nd edition, 2005.

[6] A. L. Peratt. Advances in numerical modeling of astrophysical and space plasmas. *Astrophys. Space Sci.*, 242:93–163, 1997.

[7] D. Vasileska, H. R. Khan, and S. S. Ahmed. Modeling Coulomb effects in nanoscale devices. *J. Comput. Theor. Nanosci.*, 5:1793–1827, 2008.

[8] A. M. Kriman, M. J. Kann, D. K. Ferry, and R. Joshi. Role of the exchange interaction in the short-time relaxation of a high-density electron plasma. *Phys. Rev. Lett.*, 65:1619–1622, 1990.

[9] C. K. Birdsall and A. B. Langdon. *Plasma Physics via Computer Simulation*. Adam Hilger, 1991.

[10] B. K. Ridley. *Quantum Processes in Semiconductors*. Oxford Science Publications, 4th edition, 1999.

[11] K. J. Willis, S. C. Hagness, and I. Knezevic. Terahertz conductivity of doped silicon calculated using the ensemble Monte Carlo/finite-difference time-domain simulation technique. *Appl. Phys. Lett.*, 96:062106, 2010.

[12] P. Gori-Giorgi, F. Sacchetti, and G. B. Bachelet. Analytic static structure factors and pair-correlation functions for the unpolarized homogeneous electron gas. *Phys. Rev. B*, 61:7353–7363, 2000.

[13] C.-T. Sah. *Fundamentals of solid-state electronics*. World Scientific, 1991.